



LAWRENCE
LIVERMORE
NATIONAL
LABORATORY

Satellite Re-entry Modeling and Uncertainty Quantification

M. Horsley

September 11, 2012

2012 AMOS Conference
Maui, HI, United States
September 11, 2012 through September 14, 2012

Disclaimer

This document was prepared as an account of work sponsored by an agency of the United States government. Neither the United States government nor Lawrence Livermore National Security, LLC, nor any of their employees makes any warranty, expressed or implied, or assumes any legal liability or responsibility for the accuracy, completeness, or usefulness of any information, apparatus, product, or process disclosed, or represents that its use would not infringe privately owned rights. Reference herein to any specific commercial product, process, or service by trade name, trademark, manufacturer, or otherwise does not necessarily constitute or imply its endorsement, recommendation, or favoring by the United States government or Lawrence Livermore National Security, LLC. The views and opinions of authors expressed herein do not necessarily state or reflect those of the United States government or Lawrence Livermore National Security, LLC, and shall not be used for advertising or product endorsement purposes.

Satellite Re-entry Modeling and Uncertainty Quantification

Matthew Horsley

Lawrence Livermore National Laboratory

LLNL-CONF-580132

ABSTRACT

LEO trajectory modeling is a fundamental aerospace capability and has applications in many areas of aerospace, such as maneuver planning, sensor scheduling, re-entry prediction, collision avoidance, risk analysis, and formation flying. Somewhat surprisingly, modeling the trajectory of an object in low Earth orbit is still a challenging task. This is primarily due to the large uncertainty in the upper atmospheric density, about 15-20% (1-sigma) for most thermosphere models. Other contributions come from our inability to precisely model future solar and geomagnetic activities, the potentially unknown shape, material construction and attitude history of the satellite, and intermittent, noisy tracking data. Current methods to predict a satellite's re-entry trajectory typically involve making a single prediction, with the uncertainty dealt with in an ad-hoc manner, usually based on past experience. However, due to the extreme speed of a LEO satellite, even small uncertainties in the re-entry time translate into a very large uncertainty in the location of the re-entry event. Currently, most methods simply update the re-entry estimate on a regular basis. This results in a wide range of estimates that are literally spread over the entire globe. With no understanding of the underlying distribution of potential impact points, the sequence of impact points predicted by the current methodology are largely useless until just a few hours before re-entry.

This paper will discuss the development of a set of the High Performance Computing (HPC)-based capabilities to support near real-time quantification of the uncertainty inherent in uncontrolled satellite re-entries. An appropriate management of the uncertainties is essential for a rigorous treatment of the re-entry/LEO trajectory problem. The development of HPC-based tools for re-entry analysis is important as it will allow a rigorous and robust approach to risk assessment by decision makers in an operational setting. Uncertainty quantification results from the uncontrolled re-entry of the UARS satellite will be presented and discussed.

1. INTRODUCTION

Quantifying the uncertainty in the time and location of a satellite's re-entry into the Earth's atmosphere is difficult. The forces experienced by a satellite in Low Earth Orbit result in a highly nonlinear set of dynamic equations of motion. Many of the terms are not known with certainty, due to a lack of detailed knowledge of the physical environment and the spacecraft's construction. This leads to an inherent uncertainty in the predicted re-entry time and location. Due to the complicated nature of the equations of motion, it is difficult to adequately capture this uncertainty using analytical techniques. In cases such as this, the uncertainty can be quantified through numerical simulation. The confidence in the re-entry estimate depends on the certainty of the model inputs. Uncertainty Quantification (UQ) is the practice where one tries to determine the likelihood of a particular re-entry time if some aspects of the system are not known exactly. Several methods exist to quantify the uncertainty, see [1] for a review. Of the methods discussed in [1], Monte Carlo simulation is the most developed Uncertainty Quantification method, and has a number of advantages over alternative methods. Monte Carlo methods are nonintrusive, meaning the function used in the uncertainty calculation does not have to be modified in any way, and can be treated as a black box function. Unfortunately, Monte Carlo methods are slow and typically converge asymptotically as $1/\sqrt{N}$, where N is the number of trials. However, under very modest assumptions, convergence is guaranteed.

In cases where the distributions of some of the model input parameters are not known, they can be estimated simultaneously with the re-entry time and location using a Markov Chain Monte Carlo algorithm, to be described in the following section. Essentially, a very large number of re-entry trajectory simulations can be performed. Each simulation is performed using a different acceleration model. The acceleration models, by design, cover the set of all possible accelerations experienced by the spacecraft. In order to ensure that the resulting probability distribution

adequately represents the true probability distribution, a Markov Chain can be constructed that has the target probability distribution as its equilibrium distribution. After a sufficiently large number of steps have been taken by the chain, the state of the chain can then be used to generate samples for the ensemble. The quality of the resulting probability distribution improves by running the chain for more iterations. This can be costly, so High Performance Computer (HPC)-based algorithms will be used to enable uncertainty quantification of the re-entry/LEO trajectory in near real-time. This is important as it will allow a rigorous and robust approach to risk assessment by decision makers in an operational setting

2. MARKOV CHAIN MONTE CARLO

Markov Chain Monte Carlo (MCMC) represents a general class of computing techniques that are used in a great many different fields, such as physics, chemistry, biology, and computer science. The method has been extensively discussed in the literature and has a sound theoretical foundation. For a review of the topic, many excellent tutorials exist, see [2] for an example. The goal is to construct a probability model of the satellite re-entry based on the observed data. Once constructed, the probability model can be used to estimate any statistical quantity of interest, such as the most likely re-entry time or even a Bayesian confidence region for the re-entry location. Let $\theta: (\theta_1, \dots, \theta_p)$ denote the vector of p parameters that are required for modeling the satellite's trajectory. Any prior beliefs about these parameters, before any new data is collected, is expressed using a prior probability distribution, $\pi(\theta)$. Upon collecting new data, the prior can be updated using the likelihood function, $L(D|\theta)$, where $D = (d_1, \dots, d_n)$ represents the new data collected. The updating is done using Bayes' theorem,

$$\pi(\theta|D) = \frac{\pi(\theta)L(D|\theta)}{\int_{\theta} \pi(\theta)L(D|\theta)} \quad (1)$$

where $\pi(\theta|D)$ is called the posterior distribution and represents the probability of the parameters p after the new data has been collected.

The expression in the denominator of (1) involves integration over all possible satellite trajectories. Generally, this integral is intractable and cannot be solved analytically. Thus, in most cases (including satellite re-entry), eq (1) cannot be solved exactly. However, an approximation can be computed very easily and efficiently using the MCMC method. The exact approach will be discussed below, but a very brief summary of the method is given here. The MCMC technique is used to generate a large number of satellite trajectories. Each satellite trajectory generated by the algorithm is sampled in direct proportion to its probability. Thus trajectories that are very likely will be sampled many times by the algorithm. Trajectories that are not very likely will only be sampled a few times (or not at all) by the algorithm. Once an ensemble of satellite trajectories has been generated, any sort of statistical calculation can be performed, such as computing a mean, variance or credible interval. Accuracy can be improved simply by sampling a greater number of trajectories. The importance of an efficient method for computing the satellite trajectory likelihood lies in the fact that the MCMC method will typically require a large number of iterations. Numerical integration of satellite re-entry trajectories is generally difficult and time consuming, and hence this method will require a large computer in order to generate results in a timely manner.

The method starts by defining a Markov Chain, \mathcal{M} , which will be used to generate samples from a probability distribution π on the space of all possible re-entry trajectories, Ω . By construction, \mathcal{M} will have states $\omega \in \Omega$ and a stationary distribution $\pi(\omega)$. If the current state of the chain is ω , a new state ω' will be proposed for the next step of the chain. The new state will be generated following a proposal distribution, $q(\omega, \omega')$, which is dependent on the current state of the chain. The proposed move ω' will be accepted with a probability

$$A(\omega, \omega') = \min \left(1, \frac{\pi(\omega')q(\omega, \omega')}{\pi(\omega)q(\omega', \omega)} \right).$$

By the ergodic theorem, it can be shown that \mathcal{M} will converge to its stationary distribution as long as \mathcal{M} satisfies a few requirements, such as being irreducible and aperiodic (see [3] for details). Using a uniform proposal distribution (see table 1) allows a simplification in the acceptance probability,

$$A(\omega, \omega') = \min \left(1, \frac{\pi(\omega')}{\pi(\omega)} \right).$$

The acceptance probability $A(\omega, \omega')$ now depends only on the ratio of the likelihoods, and does not require knowledge of the normalizing constant Z . This is exactly what we need. It allows us to generate a large number of re-entry trajectories in direct proportion to their probabilities, but without requiring an intractable integration over all possible trajectories. The only requirement is to compute the likelihood of a re-entry trajectory. The log likelihood function, $L(D|\theta)$, is computed by calculating the chi-squared cost between the model's semi-major axis value, a_m , and the data semi-major axis value, a_d , at the validity time of a TLE, and summing over all the data points used in the calculation:

$$\log L(D|\theta) = \sum_{i=1}^N -\frac{1}{2} \left(\frac{a_d^i - a_m^i}{\sigma} \right)^2.$$

Here, σ is the variance of the semi-major axis data. Since TLE data do not have estimates of the semi-major axis variance, this value has to be obtained from other sources. For this analysis, a value of 100 meters was found to yield good results. Each Monte Carlo trajectory is performed using a different acceleration model. The acceleration models, by design, cover the set of all possible accelerations experienced by the spacecraft. The sources of uncertainty accounted for in this analysis were related to the spacecraft's ballistic coefficient calculation, the modeling error in atmospheric density, and errors in solar and geomagnetic forecasts. Modeling the uncertainty due to the ballistic coefficient required 4 parameters, the uncertainty atmospheric density required 1 parameter (normal), and the solar activity was modeled using a different stochastic model (described in next section) for each iteration. Uncertainty in the predicted re-entry due to the geomagnetic activity uncertainty was not accounted for in this analysis. Future efforts will incorporate this source of uncertainty as well.

The Markov Chain will be simulated using the algorithm described in table 1. The probability of a particular re-entry time is estimated using

$$\hat{P}_t = \frac{1}{n_{mc} - n_{bi}} \sum_{n=n_{bi}}^{n_{mc}} \mathbb{I}(t < t_n < t + dt),$$

where \hat{P}_t is the probability of the satellite re-entering at time t , and n_{mc} and n_{bi} are the total number of Monte Carlo iterations and an initial number of discarded moves performed in the calculation, respectively. Thus the probability is obtained by simply counting the number of re-entry trajectories that contain occur between t and $t+dt$ and normalizing by the total number of iterations used in the calculation.

Table 1 MCMC algorithm for Re-entry Uncertainty Quantification. Below, $N(m, \sigma)$ refers to a random draw from a normal distribution having a mean of m and a variance of σ .

MCMC Algorithm

for iteration 1,...,N

- a. Initialize proposal trajectory using current trajectory
- b. sample U from $[1,2,3,4]$ uniformly at random
 - if** $U = 1$ **then** (Area-to-mass ratio move)

$$\frac{A}{m_{prop}} = N\left(\frac{A}{m_{curr}}, \frac{A}{m_{curr}}/10.0\right)$$
 - else if** $U = 2$ **then** (shape parameter 1 move)

$$s_{prop}^1 = N(s_{prop}^1, s_{prop}^1/10.0)$$
 - else if** $U = 3$ **then** (shape parameter 2 move)

$$s_{prop}^2 = N(s_{prop}^2, s_{prop}^2/10.0)$$
 - else if** $U = 4$ **then** (shape parameter 3 move)

$$s_{prop}^3 = N(s_{prop}^3, s_{prop}^3/10.0)$$
 - end if**
- c. compute trajectory, calculate likelihood
- d. accept/reject proposed re-entry trajectory using $A(\omega, \omega')$
- e. record resulting re-entry time, location

3. SATELLITE RE-ENTRY MODELING

This section will describe the approach used to model the satellite re-entry trajectory. A model of the acceleration experienced by a satellite is required when computing a re-entry trajectory. The acceleration model is discussed below, and includes terms due to Earth's gravity, lunar and solar perturbations, and atmospheric drag. Due to the high accuracy achievable with numerical integration, a multistep numerical integration routine was used in predicting the satellite's re-entry trajectory, see [4] for details. The integration routine was executed with a step size of 60 seconds. This step size was maintained until the spacecraft's altitude had reached 120 km, at which point the step size was decreased to 1 second. Re-entry was defined to occur at an altitude of 100 km. Once this condition was met, the integration routine was halted. The acceleration due to the Earth's gravity was modeled using the Joint Gravity Model-3 (JGM-3) at order and degree 70 [5].

Atmosphere Model

The NRLMSISE00 atmosphere model [6] was used to compute atmospheric densities, temperature and estimate the concentration of atomic oxygen. The atmospheric density was necessary for computing the drag acceleration, and the atomic oxygen concentration was used to estimate the accommodation coefficient (which was used in the drag coefficient calculation, see next section for more details). NRLMSISE00 is an empirical model of the Earth's atmosphere, and extends from the ground to the exobase. The inputs to the NRLMSISE00 model are: current year, day of year, seconds in the day, altitude, latitude and longitude, local apparent solar time, 81 day average of the F10.7 flux, daily F10.7 flux for previous day, and the daily magnetic index. The model outputs are: number densities of He, O, N₂, O₂, Ar, H, N and anomalous oxygen, the total mass density, exospheric temperature, and temperature at altitude.

The NRLMSISE00 (as well as other atmosphere models) has been shown to have errors in density on the order of 15-20% [7]. This is a significant source of uncertainty, and hence the modeled density was treated as an uncertain model parameter when computing drag. The atmospheric density was treated as a Gaussian random variable, with a mean given by the NRLMSISE00 model, and a width of 20%. This was done to generate an ensemble of atmospheres for modeling the possible drag accelerations the spacecraft might experience.

For each Monte Carlo trial performed, a random draw was made from a Gaussian distribution, denoted by g_{atmo} . This distribution had a mean of 0, and a width of 0.2. This value was then used to adjust the density for the trajectory calculation,

$$g_{atmo} = N(0,0.2)$$

$$\rho_{model} = (1 + g_{atmo})\rho_{NRLMSISE00}$$

where $N(m, s)$ is the normal distribution with a mean of m and a sigma of s , $\rho_{NRLMSISE00}$ is the density generated from the call to the NRLMSISE00 model, and ρ_{model} is the density used when computing the drag.

The oxygen concentration estimated by the NRLMSISE00 model was used to compute an estimate of the accommodation coefficient. The accommodation coefficient, α_{accom} , is a convenient measure of the interaction between the incoming atmospheric molecule and the surface of the satellite. In a sense, α_{accom} , describes how much memory the gas molecule retains of its initial velocity after its interaction with the satellite surface. Values of α_{accom} can vary from 0 to 1, and is approximately 0.9 at altitudes of 300 km [8]. Values of 1 indicate complete accommodation, meaning the emitted particle has a kinetic energy that has completely adjusted to the thermal energy of the surface. According to [9], the accommodation coefficient is related to the concentration of atomic oxygen at the altitude of the satellites, which is correlated with the Sun's effect on the Earth's atmosphere. A number of papers review accommodation at orbital altitudes and the effects on satellites (see [8, 10] and references contained therein). The semi-empirical model described in [9] will be used to estimate the accommodation

coefficient. The atomic oxygen density computed using NRLMSISE00 model will be used as input into the accommodation model. The accommodation coefficient will then be used to compute the satellite's coefficient of drag.

Solar and Geomagnetic Activity Models

The NRLMSISE00 atmosphere model requires estimates of the solar radio flux at the 10.7 cm wavelength and the geomagnetic activity index, Ap . The indices required include the daily values for the F10.7 and magnetic fluxes, as well as the 81 day F10.7 average. In order to obtain accurate estimates of the atmospheric density, it is necessary to accurately predict the future values of these indices. Unfortunately, it is difficult to accurately predict these values, and represents a significant source of uncertainty when predicting the re-entry of a spacecraft. The predicted values of both F10.7 and Ap were obtained from <http://celestrak.com/>. These estimates are in turn gotten from the National Oceanic and Atmospheric Administration (NOAA). The uncertainty in the predicted future values of the observed, daily F10.7 was modeled using a scalar exponential Gauss-Markov sequence, see [11] for details. This method allows the creation of an ensemble of realistic predictions of F10.7 which capture the daily variation around the mean prediction provided by NOAA. The Ap predicted value was used in the calculation of the atmospheric density, but was not included in the uncertainty analysis.

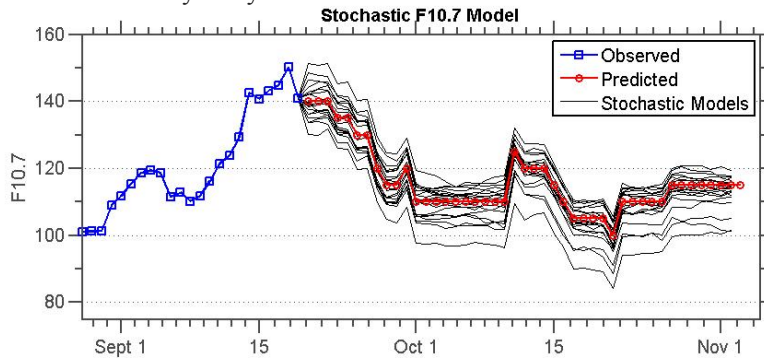


Fig. 1 Example stochastic trajectories of F10.7 using the scalar exponential Gauss-Markov sequence described in [11].

Ballistic Coefficient Model

An object traveling through the Earth's atmosphere will experience aerodynamic forces that can be decomposed into two terms, drag and lift. Drag acts in the direction of the velocity relative to the atmosphere, and lift acts in a direction which depends on the orientation of the spacecraft and is perpendicular to drag. In most cases involving LEO satellites, drag will tend to dominate (see [12, 13]). The magnitude of the acceleration due to drag can be represented by

$$a_{drag} = \frac{1}{2} \frac{A}{m} C_D \rho |\vec{v}|^2 = \frac{1}{2} B \rho |\vec{v}|^2$$

where a_{drag} is the acceleration caused by the drag acting in the direction opposite of \vec{v} , ρ is the atmospheric density, m is the mass of the satellite, \vec{v} is the velocity of the satellite with respect to the atmosphere, C_D is the coefficient of drag, and $B = C_D A/m$ is the ballistic coefficient. Here we are assuming \vec{v} to be equal to the satellite's inertial velocity, and in effect we are neglecting the component of the atmospheric velocity that co-rotates with the Earth. The coefficient of drag is used to represent the effect of momentum transfer between the satellite and the surrounding atmosphere. The coefficient depends on the satellite's shape and orientation, flow conditions and surface chemistry effects. The ballistic coefficient is expected to decrease as a function of altitude (see figure below).

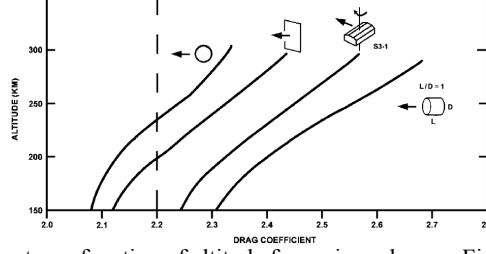


Fig 2. Drag coefficient as a function of altitude for various shapes. Figure is due to Moe [8]

In order to simulate this behavior, a physics-based model of the drag coefficient was used. At LEO altitudes where the mean free path of a gas molecule is much larger than the size of the satellite, the coefficients of drag can be computed exactly for cases involving simple shapes, like spheres, cylinders and flat plates. We will use the model described in [14] to compute the drag coefficient, which is based on Sentman's treatment of drag in free molecular flow conditions [15, 16] (with modifications due to Moe [10] in order to account for the effect of the accommodation coefficient, α_{accom} , discussed above). The ballistic coefficient was modeled in the following way.

The acceleration due to drag has terms related to the area-to-mass ratio, the spacecraft velocity, the atmospheric density, and the coefficient of drag. For this analysis, it was assumed the area-to-mass ratio was constant. In order to model the spacecraft's coefficient of drag, it was necessary to know its shape. Unfortunately, the shapes of spacecraft are oftentimes complicated, and no detailed geometry model is typically available. In order to simplify the analysis, the satellite geometry was modeled as if it were a collection of spheres, plates and cylinders when computing the coefficient of drag. Three shape parameters, s_1 , s_2 and s_3 were drawn from a uniform, random distribution between 0 and 1. An effective coefficient of drag was then computed as the weighted sum of the coefficients for a sphere, a square plate at normal incidence, and a cylinder (with its long axis aligned with the velocity vector),

$$C_d^{eff} = \frac{s_1 C_d^{sphere} + s_2 C_d^{cylinder} + s_3 C_d^{plate}}{s_1 + s_2 + s_3} .$$

As time advanced, the ballistic coefficient was modeled to slowly decrease in value as predicted by physics.

4. UARS EXAMPLE

The NASA Upper Atmospheric Research Satellite (UARS) was selected as a test case for the MCMC Re-entry Uncertainty Quantification algorithm. UARS re-entered the Earth's atmosphere at 0400 GMT on September 24, 2011 [17]. The location of the re-entry was reported by the Joint Space Operations Center at Vandenberg Air Force Base in California as 14.1 degrees South latitude and 170.2 degrees West longitude. The MCMC algorithm requires data on the satellite's semi-major axis history. This data can be obtained by using the Two-line Element (TLE) files published online through the www.space-track.org website, operated by the United States Strategic Command (USSTRATCOM). The TLE data were transformed into osculating orbital elements, from which a series of semi-major axis values were created. A total of 5 TLE files were used as input to the algorithm, spanning from the last recorded UARS TLE (approx. 90 before re-entry) to 24 hours before re-entry, spaced at roughly 12 hours apart. With this set of data, the MCMC algorithm was ran, with a random initialization of the ballistic coefficient and shape parameters. Fig. 3 below shows the convergence of the algorithm as a function of the number of iterations performed. The ballistic coefficient can be seen to converge to a mean value of approximately $0.0091 \text{ m}^2 / \text{kg}$ with a standard deviation of $0.0003 \text{ m}^2 / \text{kg}$.

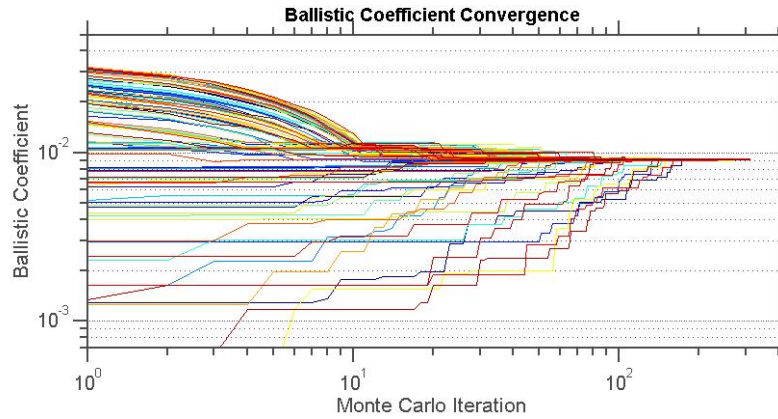


Fig. 3. A large number of Markov Chains were initialized at different values of ballistic coefficient and shape parameters. The MCMC algorithm described in table 1 was executed for 300 iterations. The ballistic coefficient sampled by each chain converged to a value of 0.0091 by 150 iterations.

Fig. 4 below shows the distribution of re-entry times computed using the MCMC Re-entry UQ algorithm. The most likely re-entry time was computed to be 09/24/2011 04:16:1.8 UTC, with a standard deviation of 0.61 hours. The distribution is not symmetric, and shows a long tail towards later re-entry times. Figure 5 shows the distribution of re-entry locations. The density of points plotted on the map indicates the relative probability of the satellite re-entering at the indicated position. The actual re-entry location is contained in the left-most tail of the distribution.

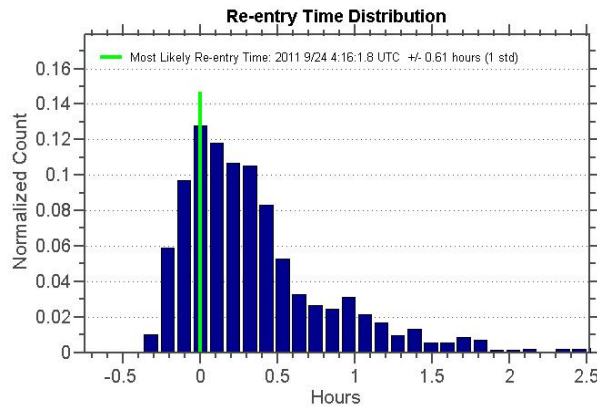


Figure 4 Distribution of re-entry times computed using MCMC UQ. A total of 5 TLE files were used as input to the algorithm, spanning from the last recorded UARS TLE (approx. 90 before re-entry) to 24 hours before re-entry.

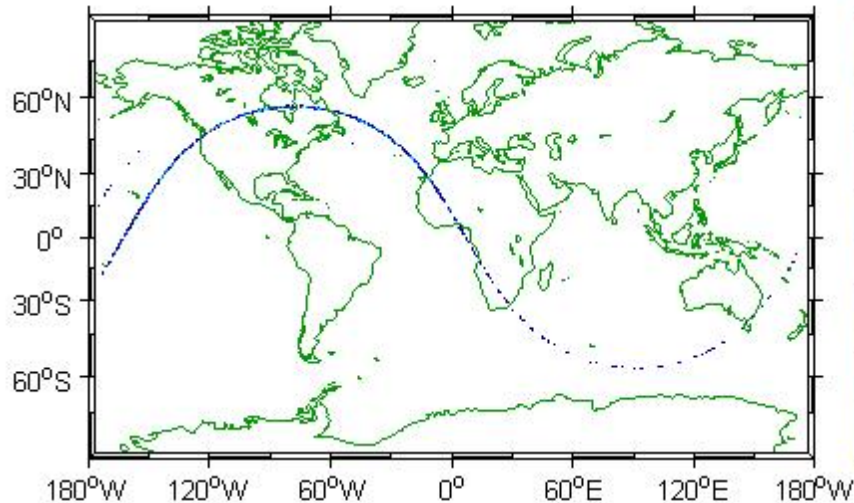


Figure 5 Distribution of re-entry locations. The density of points indicates the relative probability of the particular location. The actual re-entry location (14.1 S, 170.9 W) lies in the tail of the predicted distribution. The sparse distribution of points in the right hand side of the distribution is due to lack of sufficient statistics.

5. CONCLUSION

Estimating the uncontrolled re-entry of a satellite is difficult due to the uncertain nature of the modeling required to compute a trajectory. The uncertain nature of the re-entry reduces the utility of a point estimate and emphasizes the benefits of a robust estimate of the uncertainty. A simple method of quantifying this uncertainty was introduced that did not require knowledge of hard to obtain data, such as satellite geometry and ballistic coefficient. A data-driven, Markov Chain Monte Carlo approach to Uncertainty Quantification was described and demonstrated on the UARS satellite. Performance was good in cases involving more than 150 MCMC iterations. A simple procedure was described for diagnosing convergence of the MCMC algorithm and showed good performance in the case of the UARS satellite re-entry.

6. ACKNOWLEDGEMENTS

This work performed under the auspices of the U.S. Department of Energy by Lawrence Livermore National Laboratory under Contract DE-AC52-07NA27344.

7. REFERENCES

1. Xiu, Hesthaven, "High Order Collocation Methods for Differential Equations with Random Inputs", SIAM J. Sci. Comput., Vol 27, No 3 2005
2. Tierney, L., "Markov Chains for Exploring Posterior Distributions", The Annals of Statistics, vol. 22, no 4 1994
3. Roberts, G., "Markov chain concepts related to sampling algorithms", in *Markov Chain Monte Carlo in Practice*, ser. Interdisciplinary Statistics Series. Chapman and Hall, 1996.
4. O. Montenbruck, and E. Gill, "Satellite Orbits", Springer, (2001)
5. Tapley B., Watkins M., Ries J., Davis G., Eanes R., Poole S., Rim H., Schultz B., Shum C., Nerem R., Lerch F., Marshall J., Klosko S., Pavlis N., Williamson R., "The Joint Gravity Model 3," *J. Geophys. Res.* 101(B12):28029-28049.

6. M. Picone, A.E. Hedin, D.P. Drob, and A.C. Aikin, "NRL-MSISE-00 Empirical Model of the Atmosphere: Statistical Comparisons and Scientific Issues," *J. Geophys. Res.*, doi:10.1029/2002JA009430, (2003).
7. Marcos, F.A., "Accuracy of atmospheric drag models at low satellite altitudes," *Advances in Space Research*, 10, 417, 1990
8. Moe, K., Moe, M., "Gas-surface interactions and satellite drag coefficients", *Planetary and Space Science*, Vol. 53, 2005, pp. 793–801. DOI: 10.1016/j.pss.2005.03.005
9. Pilinski, M., Argrow, B., and Palo, S., "Semiempirical Model for satellite Energy-Accommodation Coefficients", *J. of Spacecraft and Rockets*, Vol. 47, No 6, 2010. DOI: 10.2514/1.49330
10. Moe, K., Moe, M., Wallace, S., "Improved Satellite Drag Coefficient Calculations from Orbital Measurements of Energy Accommodation", *J. of Spacecraft and Rockets*, Vol. 35, No. 3, 1998, pp. 266–272. DOI: 10.2514/2.3350
11. Woodburn, J., Lynch, S., "A Numerical Study of Orbit Lifetime", AAS 05-297
12. Moore, P., "The Effect of Aerodynamic Lift on Near Circular Satellite Orbits", *Planet. Space Sci.*, Vol 33, No 5, pp 479-491, 1985
13. Roy, A.E., *Orbital Motion*, Fourth Edition. Taylor & Francis (2005).
14. Sutton, E., "Effects of Solar Disturbances on the Thermosphere Densities and Winds from CHAMP and GRACE satellite Accelerometer Data," Ph.D. Dissertation, Aerospace Engineering Sciences, Univ. of Colorado, Boulder, 2008
15. Sentman, L H, "Comparison of the Exact and Approximate Methods for Predicting Free Molecule Aerodynamic Coefficients," *ARS Journal*, 1576-1579 (1961)
16. Sentman, L H, "Effect of Degree of Thermal Accommodation on Free Molecule Aerodynamic Coefficients," *ARS Journal*, 1408-1410 (1962a)
17. http://www.nasa.gov/mission_pages/uars/index.html